RhoD regulates endosome dynamics through Diaphanous-related Formin and Src tyrosine kinase

Stéphane Gasman*†, Yannis Kalaidzidis‡ and Marino Zerial*§

*Max Planck Institute for Molecular Cell Biology and Genetics, Pfotenhauerstrasse 108, Dresden D-01307, Germany
†CNRS UPR-2356 Neurotransmission et Sécrétion Neuroendocrine, 5 rue Blaise Pascal, 67084 Strasbourg, France
‡A.N. Belozersky Institute of Physico-chemical Biology, Build A, Moscow State University, Moscow 119899, Russia
§e-mail: zerial@mpi-cbg.de

Published online: 10 February 2003; DOI: 10.1038/ncb935

Early endosomes move bidirectionally between the cell periphery and the interior through a mechanism regulated by the low molecular weight GTPase RhoD. Here, we identify a novel splice variant of human Diaphanous, hDia2C, which specifically binds to RhoD and is recruited onto early endosomes. Expression of RhoD and hDia2C induces a striking alignment of early endosomes along actin filaments and reduces their motility. This activity depends on the membrane recruitment and activation of c-Src kinase, thus uncovering a new role in endosome function. Our results define a novel signal transduction pathway, in which hDia2C and c-Src are sequentially activated by RhoD to regulate the motility of early endosomes through interactions with the actin cytoskeleton.

Endocytosis is a highly dynamic process responsible for many cellular functions, such as the uptake of essential nutrients and growth factors[1]. Endocytosed molecules are transported into early endosomes from where they are either recycled to the surface or delivered to degradative compartments. Early endosomes are highly dynamic organelles; they fuse with clathrin-coated vesicles and also with each other, modify their geometry through membrane fission and tubulation, move over long distances and transfer cargo to other organelles. These properties require the dynamic association of endosomes with the actin and microtubule cytoskeleton. Actin and various myosin motors function in the internalization from the plasma membrane[2–4] and facilitate the delivery of cargo to degradative compartments[5,6]. Actin filaments have been proposed to propel endocytic vesicles in the cytoplasm[7]. Interactions with microtubules and microtubule motors are necessary for the positioning of endocytic organelles[8–10], for the transport of cargo from early to late endosomes and for transcytosis in polarized epithelial cells[11,12].

Whereas the participation of the cytoskeleton and associated motors is well established, very little is known about the membrane factors regulating endosome movement and distribution. Both the Rab and Rho families of low molecular weight GTPases are involved in this process. In addition to its function as a regulator of endocytosis, membrane tethering and fusion[13], Rab5 also stimulates the motility of early endosomes on microtubules, presumably through kinesin-like motor proteins[10]. Rho proteins regulate diverse functions, such as cell adhesion, cell cycle, transcription, cell polarity and membrane trafficking[14]. In endocytosis, RhoA and Rac are involved in receptor uptake[15] and Cdc42 regulates polarized internalization at the basolateral side of epithelial cells[16]. To date, RhoD has a unique function among Rho family members in that it regulates the motility of early endosomes[17]. RhoB is mainly associated with late endosomes and is involved in transport to lysosomes[18]. Several functionally distinct Rho effectors have been identified[19], including Diaphanous-related Formin proteins (DRFs). For example in yeast, Bn1p binds to Rho1p and Cdc42p[20,21]. In mammals, mDia1 binds RhoA, mDia2 both RhoA and Cdc42 (refs 22, 23) and Rac1 interacts with both FHOS (formin homologue overexpressed in spleen) and FRL (formin-related gene in leukocytes)[24,25]. DRFs modulate cytoskeletal organization during cytokinesis, cell polarity and spindle positioning[26,27]. Interestingly, mDia1 and mDia2 have been detected in endosomes, but the functional significance of this localization is unclear.

Whereas the effectors of Rho, Rac and Cdc42 have been extensively investigated, little is known for other Rho family members. The aim of the present work was to investigate the mechanism of RhoD action in early endosome motility.

Table 1 Effect of RhoD and hDia2C on Rab5–endosome velocity in HeLa cells.

Velocity (μm s^{-1})	Control	$RhoD^{G26V}$	hDia2C	ΔGBD-hDia2C	GBD-hDia2C	mDia1
0.1–0.4	16.0 ± 2.8	22.2 ± 1.9*	15.3 ± 0.7	29.5 ± 4.4**	15.8 ± 0.4	17.2 ± 4.2
0.4–0.8	47.4 ± 3.2	59.0 ± 5.3	45.0 ± 1.6	52.6 ± 5.9	48.0 ± 3.3	46.1 ± 5.2
0.8–1.2	18.4 ± 2.8	8.6 ± 3.9*	22.7 ± 2.0	8.1 ± 2.3*	21.0 ± 2.6	16.4 ± 4.2
1.2–1.6	7.1 ± 1.8	4.6 ± 0.9	8.6 ± 1.0	4.0 ± 1.8	7.4 ± 2.3	6.6 ± 2.3
1.6–2.0	3.5 ± 0.9	0.9 ± 1.0	3.1 ± 0.3	1.9 ± 1.0	3.4 ± 0.3	4.4 ± 1.2
>2.0	7.6 ± 4.8	4.7 ± 1.8	3.5 ± 0.6	3.9 ± 2.0	4.4 ± 1.7	9.3 ± 5.0

Numbers represent the percentage of endosomes moving at the corresponding velocity. Quantifications of independent videos were pooled to provide an average estimation of endosome motility.
*$0.05<P<0.1$; **$0.01<P<0.02$ when tested by Student's *t* test.

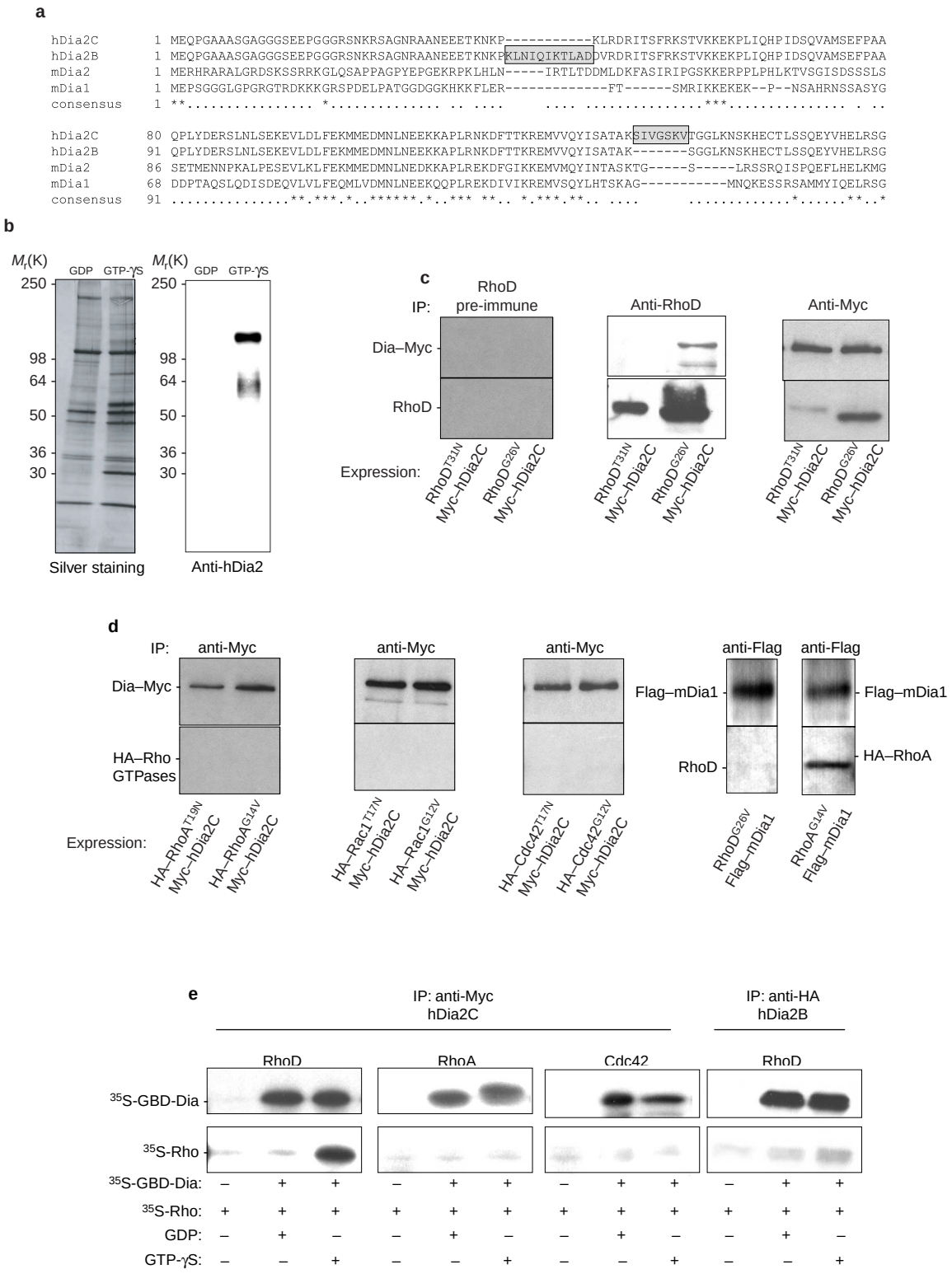

Figure 1 **hDia2C, a new member of the Formin-Related family, is a RhoD effector. a**, Alignment of the N-terminal part of hDia2C with other DRF proteins. In the CLUSTALW alignment of hDia2C, hDia2B-12C, mDia1 and mDia2, the insertion at position 149 of hDia2C and the deletion after amino-acid 42 of human Dia2-12C are framed. **b**, Interaction of hDia2C with RhoD-GTP-γS assessed by affinity chromatography. Affinity columns containing immobilized GST–RhoD-GDP and GST–RhoD-GTP-γS were incubated with human placenta cytosol. Bound proteins were eluted and analysed by silver staining and immunoblotting with affinity purified anti-hDia2 peptide antibodies. **c**, **d**, HeLa cells were cotransfected with the indicated plasmids, lysed and the expressed proteins immunoprecipitated (IP) with the indicated antibodies before detection by immunoblotting. On average, 65% of total RhoD co-immunoprecipitated with Myc–hDia2C. **e**, 35S-methionine-labelled, *in vitro*-translated wild-type RhoD, RhoA or Cdc42 were loaded with either GDP or GTP-γS and then individually mixed with the *in vitro*-translated Myc–GBD of hDia2C or HA–GBD of hDia2B. Immunoprecipitated proteins were analysed by SDS–PAGE and autoradiography.

Results

Identification and cloning of a RhoD effector protein. To search for downstream effectors of RhoD, a fusion of RhoD^{G26V}ΔCLAAT, a mutant defective in GTP hydrolysis and deleted in the carboxy-terminal isoprenylation motif, to the LexA DNA-binding protein was used to screen a HeLa cDNA library using the yeast two-hybrid system. Screening of 2×10^6 yeast transformants yielded 25 positive (His3$^+$/β-galactosidase$^+$) clones, of which five had high β-galactosidase activity (data not shown). The remaining clones were single isolates and were not pursued further. All five clones encoded a novel splice variant of hDia2, the longest matching the sequence of one of the two splice variants of hDia2B between residue 32 and 1093 (stop codon; exon 12C; EMBL accession number NP_009293). However, differing from hDia2B, the cDNA had a deletion of 11 (43–53 of hDia2B exon 12C and 156) and an insertion of seven amino acids (149–155) in the amino-terminal part containing the GTPase-binding domain, GBD (Fig. 1a). We named this new isoform of Diaphanous, hDia2C.

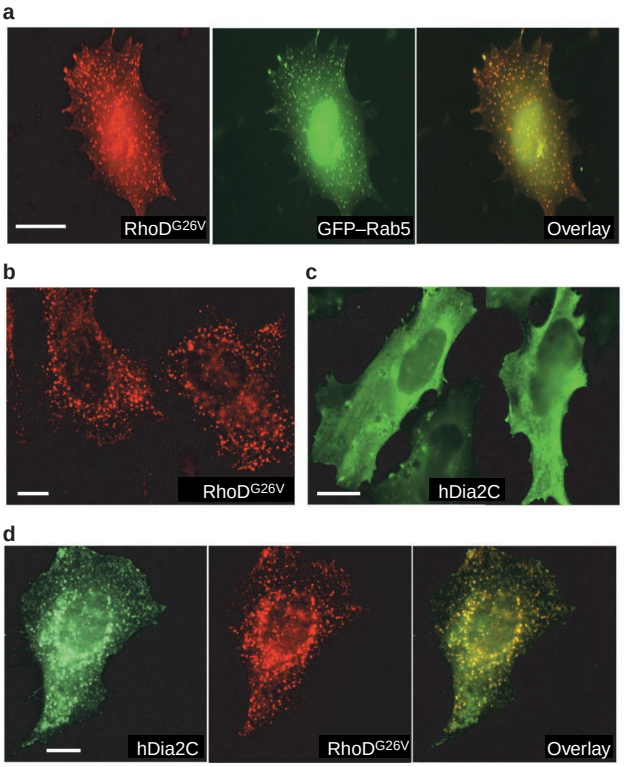

Figure 2 **The GTPase-deficient mutant RhoD^{G26V} targets hDia2C on endosomes.** HeLa cells were transfected with RhoD^{G26V} (**b**), Myc–hDia2C (**c**) or cotransfected with RhoD^{G26V} and GFP–Rab5 (**a**) or RhoD^{G26V} and Myc–hDia2C (**d**). Cells were then processed and analysed for immunofluorescence microscopy. Scale bar represents 10 μm.

Both the insert and deletion in hDia2C could be readily identified in the human EST database by BlastN and TBlastN searches. The expression of the mRNA coding for hDia2C was confirmed by reverse transcription (RT)-PCR and DNA sequencing, excluding any possibility that the assembled full-length coding sequence is a cloning artefact. Human Dia2C shares approximately 55% identity with the mouse homologues p140mDia1 and p134mDia2 (Fig. 1a) and its C terminus shares approximately 70% identity with mDia3 (data not shown). Analysis of the genomic organization of the human *Dia2* gene using Artemis software[28] revealed that amino acids 43–53 of hDia2–12C and hDia2–156, as well as the amino acids in the insertion at position 149, are encoded by separate, intermediate exons. Thus, *hDia2C* probably represents a differential splice variant of the *hDIA2* gene.

***In vivo* and *in vitro* interaction between RhoD and hDia2C.** The interaction between RhoD and hDia2C was validated through an independent biochemical approach using affinity chromatography. Recombinant glutathione *S*-transferase (GST)–RhoD was immobilized on glutathione beads, subjected to nucleotide exchange with either GDP or the non-hydrolysable GTP analogue GTP-γS[29] and incubated with human placenta cytosol. Several protein bands were specifically recovered in the GST–RhoD-GTP-γS eluate (Fig. 1b). Using anti-hDia2 antibodies in western blot analysis, we found that human Dia2 specifically eluted from the matrix of GST–RhoD loaded with GTP-γS, but not with GDP (Fig. 1b). The antibody staining could not discriminate between hDia2B and hDia2C. Nevertheless, combined with the yeast two-hybrid analysis, these chromatography data suggest that the association of hDia2C with RhoD is both specific and GTP-dependent. This interaction was next confirmed *in vivo*. In HeLa cells cotransfected with expression plasmids encoding Myc–hDia2C and RhoD^{G26V}, Myc–hDia2C co-immunoprecipitated with anti-RhoD antibodies, but not with control pre-immune serum (Fig. 1c). Conversely, RhoD co-immunoprecipitated with Myc–hDia2C. In contrast, no co-immunoprecipitation was detected in cells co-expressing Myc–hDia2C and RhoD^{T31N}, a mutant that exists predominantly in the GDP-bound form, indicating that hDia2C also interacts preferentially with RhoD-GTP *in vivo*.

Next, we wondered if hDia2C interacts specifically with RhoD. We tested whether hDia2C can interact with other Rho family members and, conversely, whether RhoD can interact with other Dia proteins. Neither activated RhoA^{G14V}, Rac1^{G12V} or Cdc42^{G12V} mutants, nor the corresponding inactive RhoA^{T19N}, Rac1^{T17N} or Cdc42^{T17N} mutants co-immunoprecipitated with Myc–hDia2C (Fig. 1d). Whereas haemagglutinin (HA) tagged RhoA^{G14V} co-immunoprecipitated with Flag-tagged p140mDia1 in cells co-expressing Flag–p140mDia1 and RhoD^{G26V}, the RhoD protein failed to co-immunoprecipitate with

Table 2 Effect of RhoD^{G26V} and ΔGBD-hDia2C on Rab5-positive endosome velocity in *Src*$^{+/+}$ and *Src*$^{-/-}$ cell lines.

	Src$^{+/+}$			Src$^{-/-}$		
Velocity (μm s^{-1})	Control	RhoD^{G26V}	ΔGBD-hDia2C	Control	RhoD^{G26V}	ΔGBD-hDia2C
0.1–0.4	18.9 ± 1.2	30.0 ± 1.4***	33.3 ± 5.6**	17.0 ± 5.4	19.0 ± 0.6	17.6 ± 4.2
0.4–0.8	50.4 ± 0.9	49.8± 4.2	45.5 ± 5.6	52.4 ± 3.6	49.0 ± 5.0	49.2 ± 3.5
0.8–1.2	15.0 ± 2.5	5.3± 4.7*	7.7 ± 5.4	16.0 ± 3.3	14.4 ± 1.6	15.2 ± 1.5
1.2–1.6	5.2 ± 1.4	5.4 ± 3.9	3.1 ± 1.6	4.5 ± 2.1	4.5 ± 2.3	4.7 ± 0.9
1.6–2.0	2.9 ± 0.6	3.5 ± 1.0	2.4 ± 1.0	2.2 ± 1.0	4.6 ± 0.5	4.0 ± 1.4
>2.0	7.6 ± 3.7	6.0 ± 4.8	8.0 ± 5.0	7.9 ± 1.2	8.5 ± 3.4	9.3 ± 5.0

Numbers represent the percentage of endosomes moving at the corresponding velocity. Quantification of independent videos were pooled to provide an average estimation of endosome motility.
*$0.05<P<0.1$; **$0.01<P<0.02$; *** $P<0.001$ when tested by Student's *t* test.

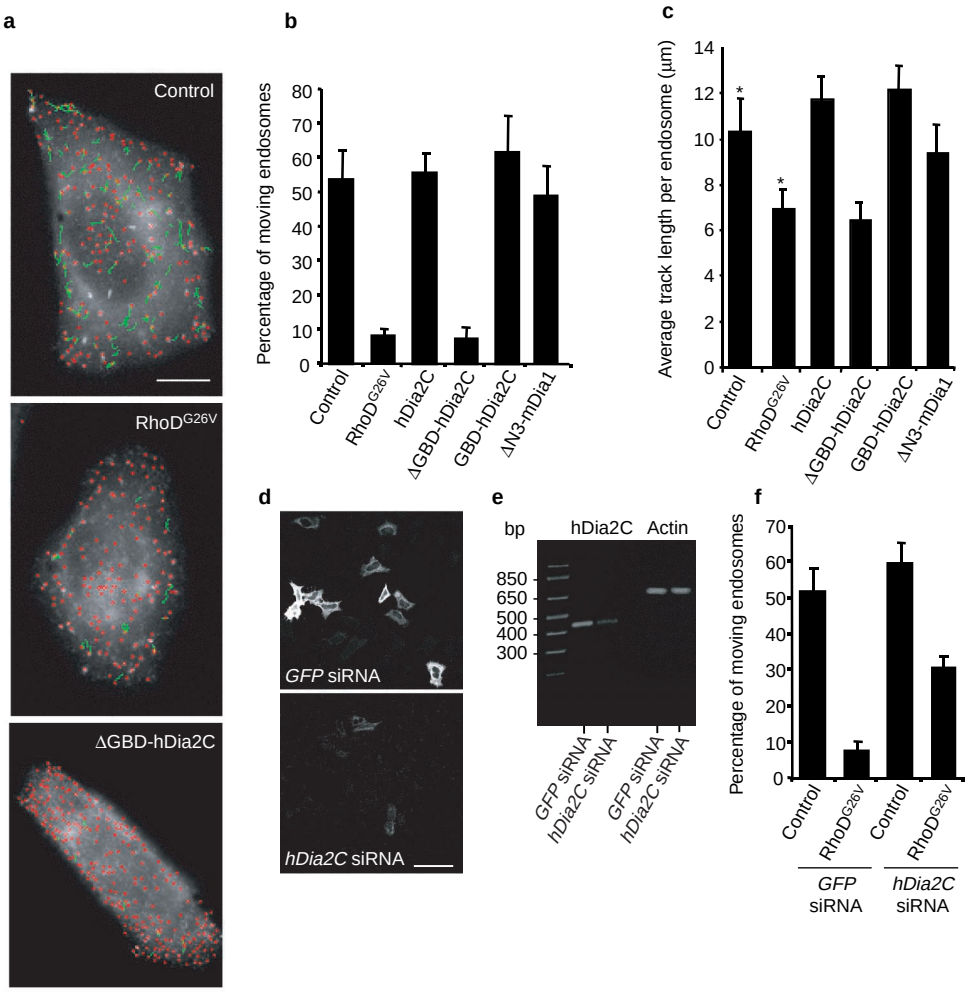

Figure 3 **RhoD and hDia2C regulate endosomes motility *in vivo*. a**, Images representing GFP–Rab5-labelled endosomes (red open circles) and tracks (green lines) in control HeLa cells, and cells expressing RhoD^{G26V} or ΔGBD-hDia2C. Movement of Rab5-GFP-positive endosomes was observed by time-lapse fluorescence video microscopy and analysed using the Motion Track program version 0.9. The tracking images of control cells, cells expressing RhoD^{G26V} and ΔGBD-hDia2C correspond to Supplementary Information, Movies 1–3, respectively. Scale bar represents 10 μm. **b**, RhoD^{G26V} and ΔGBD-hDia2C decrease the proportion of motile endosomes. The histogram represents the quantification of motile endosomes out of total endosomes and is expressed as a percentage. Note that the algorithm used in Motion Track 0.9 eliminates random trajectory movement. Each value represents an average quantification of 25 independent pooled videos. Error bars represent standard deviations. **c**, Endosome movements are reduced by RhoD^{G26V} and ΔGBD-hDia2C. Using Motion Track 0.9, the average track-length of moving endosomes was calculated. Asterisk, $P < 0.01$ when tested by Student's *t* test. **d**, Exogenous expression of Myc–hDia2C is inhibited by specific siRNA. HeLa cells were cotransfected with a plasmid encoding Myc–hDia2C and 50 nM *hDia2C* siRNA or control *GFP* siRNA. After 48 h, cells were analysed by immunofluorescence confocal microscopy. Scale bar represents 50 μm. **e**, Specific siRNA reduced the level of endogenous *hDia2C* mRNA. Total mRNA from cells expressing *hDia2C* siRNA or control *GFP* siRNA for 72 h was estimated by quantitative RT-PCR. **f**, hDia2C is required for appropriate control of endosome dynamics. Cells expressing either *hDia2C* siRNA or control *GFP* siRNA and pcDNA3.1 (control) or RhoD^{G26V} were allowed to internalize Alexa-568-labelled transferrin for 10 min. The histogram represents the quantification of motile endosomes out of all detected endosomes expressed as a percentage.

anti-Flag. These results demonstrate that hDia2C interacts specifically with RhoD. After comparison with other Dia isoforms, such specificity is most probably conferred by the sequence insertion and/or deletion within the GBD. Using *in vitro*-translated proteins, we examined the specificity of the hDia2C GBD for RhoD, RhoA and Cdc42 and compared it with that of hDia2B. Of the three Rho proteins tested, only RhoD-GTP efficiently co-immunoprecipitated with the GBD of hDia2C (Myc–GBD-hDia2C(1–287)), whereas only background levels were recovered with the GBD of hDia2B (Myc–GBD-hDia2B(1–291); Fig. 1e). These results strongly suggest that the specificity of the interaction of hDia2C with RhoD is conferred by the unique amino-acid sequence of its GBD.

RhoD recruits hDia2C onto early endosomes. To explore the functional consequence of this interaction, we began by examining the intracellular localization of hDia2C with respect to RhoD. First, we confirmed that, as previously established for Myc-tagged RhoD[17], the untagged protein has the same intracellular distribution. Using a polyclonal rabbit antiserum against recombinant RhoD, untagged RhoD^{G26V} was detected on vesicular structures containing transferrin receptor (data not shown) and green fluorescent protein (GFP)-tagged Rab5 (Fig. 2a, b). The localization of endogenous RhoD was confirmed by western blotting of an early endosome-enriched fraction from HeLa cells (data not shown). Second, as the association of Rho with Diaphanous causes a conformational change by disrupting its intra-molecular interactions[30], we tested whether the interaction with RhoD triggers the recruitment

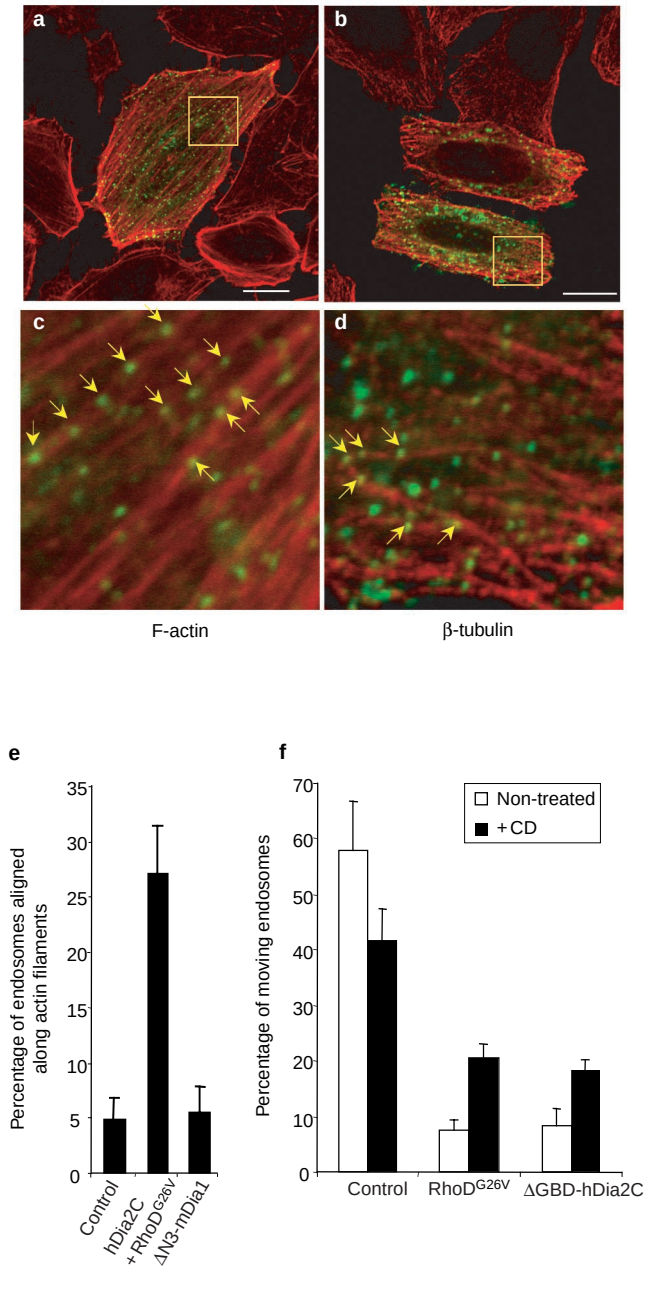

Figure 4 **RhoD and hDia2C regulate endosome–cytoskeleton interactions.** **a–d**, Endosome alignment along actin and tubulin filaments. Hela cells were cotransfected with RhoD^{G26V} and Myc–hDia2C plasmids and analysed by immunofluorescence confocal microscopy. Myc–hDia2C was detected with mouse monoclonal 9E10 anti-Myc and Cy2-conjugated anti-mouse secondary antibodies, F-actin was visualized by staining with TRITC-conjugated phalloidin (**a**, **c**), microtubules were detected with anti-β-tubulin and Cy3-conjugated goat anti-mouse antibodies (**b**, **d**). **c** and **d** represent a higher magnification of the region framed in **a** and **b**, respectively, where the arrows represent linear tracks of hDia2C-positive endosomes associated with actin filaments and microtubules, respectively. Scale bar represents 10 μm. **e**, Quantification of endosome alignment along actin filaments. Endosomes aligned along actin filaments were counted in magnified areas of cells expressing GFP–Rab5 (control), hDia2C and RhoD, or ΔN3-mDia1 ($n = 7$). **f**, Cytochalasin D partially reverses the RhoD/hDia2C-induced inhibition of endosome movement. HeLa cells were treated with 0.5 μg ml^{-1} cytochalasin D and processed for time-lapse video microscopy. The histogram represents the quantification of motile endosomes out of all detected endosomes expressed as a percentage.

of hDia2C to early endosomes. Whereas Myc–hDia2C alone was predominantly cytosolic (Fig. 2c), when co-expressed with RhoD^{G26V} it extensively colocalized on early endosomes (Fig. 2d). Consistent with the pattern of biochemical interactions, no colocalization could be detected between Myc–hDia2C and RhoA^{G14V}, Rac1^{G12V} or Cdc42^{G12V} (data not shown). These results indicate that hDia2C interacts with the GTP-bound form of RhoD and is recruited by this GTPase onto the early endosome membrane.

Both RhoD and hDia2C regulate endosome motility *in vivo*. As a potential RhoD effector, hDia2C may function in the pathway through which RhoD regulates endosome motility[17,31]. The effects of constitutively active and inactive mutants of hDia2C were compared with the effects of RhoD on the motility of endosomes labelled by GFP–Rab5 under conditions where the low expression levels of the GTPase does not affect endosome fusion and motility[32]. Approximately 90% of the transfected cells expressed both GFP–Rab5 and the mutated protein. We used a new Motion Track 0.9 computer program that detects the vesicular structures in each frame of the video sequence and groups them into tracks (see Methods). Figure 3a shows examples of GFP–Rab5 endosomes tracking images corresponding to movies 1–3 included in Supplementary Information. Data from 20–30 independent movies (30 s, 100 frames per video at 300-ms intervals) were pooled to provide a quantitative assessment of the average endosome motility. Endosome movement was bidirectional and exhibited both short- and long-range motility[10]. Compared with control cells, three distinct parameters were affected by the RhoD mutant. First, expression of RhoD^{G26V} markedly decreased the number of motile endosomes. Whereas in control cells 53.4 ± 8.7% of GFP–Rab5-labelled endosomes were motile during the imaging time, this fraction decreased to only 7.7 ± 2% in cells expressing RhoD^{G26V} (Fig. 3a, b; also see Supplementary Information, Movies 1, 2). Second, in agreement with previous data[31], the average track length per moving endosome was decreased by ~33% (6.9 μm per track versus 10.3 μm per track in control cells; Fig. 3c). Third, the velocity of early endosome movement was reduced (Table 1). Approximately half of the population of endosomes moved at a speed ranging between 0.4 and 0.8 μm s^{-1}. Whereas the proportion of endosomes moving at low speed increased, that of endosomes moving at high speed decreased in RhoD^{G26V} -expressing cells. Altogether, RhoD not only slows the velocity of endosome movement[17,31], but also imposes a marked block (85%) on motility.

We next tested the effects of full-length hDia2C and an activated mutant lacking the amino-terminal GBD (ΔGBD-hDia2C). A similar truncation renders the activity of mDia1 and Bni1p independent of the interaction with the GTPase[20,30]. ΔGBD-hDia2C mainly colocalized with GFP–Rab5 on endosomes (data not shown), implying that deletion of the GBD bypasses the recruitment step by RhoD, allowing the constitutively active protein to interact with other factors on the early endosome membrane. Remarkably, similar to what observed for RhoD, expression of ΔGBD-hDia2C blocked ~85% of endosomes in a non-motile state (Fig. 3a, b; also see Supplementary Information, Movie 3). Moreover, the average track length per moving endosome was reduced by 38% (Fig. 3c and Table 1). These parameters were unaffected by expression of full-length hDia2C, consistent with accumulation of the protein in cytosol in the absence of RhoD (Fig. 2c). In addition, no significant effects were also observed after expression of a mutant containing the GBD domain but lacking the functional FH domains (Fig. 3b, c and Table 1). To check for specificity, ΔN3-mDia1, the corresponding activated mutant of the RhoA-regulated DRF, p140mDia1 (ref. 30), was expressed in HeLa cells. These cells displayed a normal proportion of motile endosomes (Fig. 3b), which moved at a similar speed to control cells (Fig. 3c and Table 1), arguing that the effects of hDia2C on endosome motility are specific. Similar to RhoD[17], overexpression of hDia2C did not cause any detectable block of transferrin uptake. The data so far presented establish a strong correlation between the activity

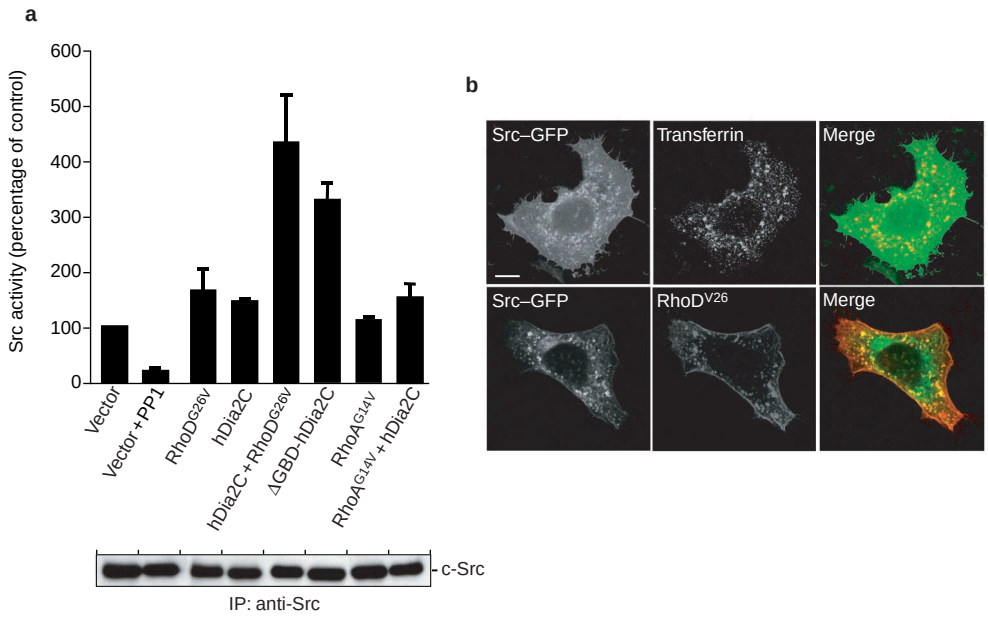

Figure 5 **hDia2C stimulates Src-kinase activity in HeLa cells. a**, HeLa cells were transfected with plasmids encoding the indicated proteins and cell lysates were immunoprecipitated with anti-Src antibodies and subjected to kinase assay. Results (means ± sem, $n = 3$) are expressed as percentage of control values from HeLa cells transfected with empty vector. The amount of c-Src immunoprecipitated in each experiment was visualized by immunoblotting. **b**, Cells expressing c-Src–GFP were allowed to internalize Alexa-568-labelled transferrin for 30 min (top) or were cotransfected with Myc–RhoD^{G26V} (bottom) and processed for immunofluorescence microscopy. Scale bar represents 10 μm.

of RhoD and hDia2C in endosome motility. To demonstrate that the function of hDia2C lies downstream of RhoD, we employed RNA interference (RNAi)[33] to inhibit the expression of endogenous hDia2C and rescue the effect of RhoD on endosome motility. Short interfering RNA oligonucleotides (siRNA) corresponding to the specific insertion found in the 5′ region of *hDia2C* mRNA were transfected into HeLa cells. We verified that *hDia2C* siRNA efficiently blocked the expression of Myc-tagged *hDia2C* by immunofluorescence microscopy (Fig. 3d) and reduced the expression of endogenous *hDia2C* mRNA by ~60%, as determined by quantitative RT-PCR (Fig. 3e). Expression of *hDia2C* siRNA reversed the inhibitory effect of RhoD^{G26V} on endosome motility proportionally to the reduction in *hDia2C* mRNA (Fig. 3f). In the presence of *hDia2C* siRNA, the inhibitory effect of RhoD^{G26V} on the percentage of motile endosomes was diminished by ~50%, whereas an unrelated siRNA had no effect (Fig. 3f).

These inhibitory effects suggest that RhoD and hDia2C can regulate the association of endosomes with and/or movement along actin filaments and microtubules. Co-expression of RhoD^{G26V} and Myc–hDia2C in HeLa cells induced similar effects to those previously observed after expression of mDia1 (ref. 34); that is, cells elongated, displayed an increase in stress fibre content (Fig. 4a) and an alignment of microtubules parallel to the cell axis (Fig. 4b). In addition, however, we observed a striking alignment of hDia2C-positive endosomes along actin filaments (Fig. 4c). Neither hDia2C (Fig. 4d) nor mDia1 (see Supplementary Information, Fig. S1) promoted a similar alignment of early endosomes on microtubules. We estimated (Fig. 4e) that hDia2C enhances the proportion of early endosomes aligned along actin filaments by ~400%, whereas in cells expressing ΔN3-mDia1 as a control, no alterations were observed, arguing that the effect induced by hDia2C is specific. Treatment of cells with the actin depolymerizing drug cytochalasin D reduced the inhibitory effect of RhoD^{G26V} and ΔGBD-hDia2C on the percentage of motile endosomes to 50% and 56%, respectively (Fig. 4e). This supports the proposal that RhoD and hDia2C could modulate endosome motility, at least partially, by stabilizing their association with the actin cytoskeleton.

hDia2C stimulates Src-kinase activity in HeLa cells. Earlier studies demonstrated a functional association of mDia-1, -2 with Src kinase[35]. We tested whether this applies also to RhoD/hDia2C, particularly in light of the previously reported association of c-Src with endosomal structures[36]. Immunoprecipitated c-Src from HeLa cells expressing RhoD^{G26V}, hDia2C or both, was subjected to a kinase assay measuring phosphorylation of a specific c-Src peptide substrate. Addition of the Src inhibitor PP1 (5 μM) decreased the kinase activity by more than 80%, demonstrating the specificity of the assay (Fig. 5). Expression of RhoD^{G26V} or hDia2C had a moderate stimulatory effect on c-Src activity (164 ± 40% and 145 ± 6.5%, respectively) when compared with control. However, a potent stimulation of c-Src kinase was induced by co-expression of both RhoD^{G26V} and hDia2C (432 ± 88%) and by the activated ΔGBD-hDia2C mutant (325 ± 38.5%). Neither expression of RhoA^{G14V} alone nor co-expression with hDia2C stimulated c-Src kinase activity (150 ± 28%), compared with hDia2C alone. Interestingly, the stimulation of kinase activity by RhoD^{G26V} was accompanied by an enhanced recruitment of c-Src onto endosomes when compared with control cells, where c-Src was mainly cytosolic (Fig. 5b). Collectively, these data suggest that, after recruitment and activation by RhoD-GTP, active hDia2C can recruit c-Src on the early endosome membrane and stimulate its kinase activity.

The effects of RhoD/hDia2C on endosome motility require c-Src. The activation of c-Src by RhoD and hDia2C may be functionally required for endosome motility or may have another purpose in the context of this organelle. Not surprisingly, expression of activated Src^{Y527F}–GFP alone had no effect on endosomes motility (data not shown), consistent with the cytosolic localization of the protein in the absence of concomitantly expressed RhoD (Fig. 5). To test the requirement for c-Src function in the RhoD/hDia2C-induced inhibition of endosome motility, we used *Src*$^{-/-}$ cells derived from a knock-out mouse embryo[37]. Both *Src*$^{-/-}$ and *Src*$^{+/+}$ cells were assayed

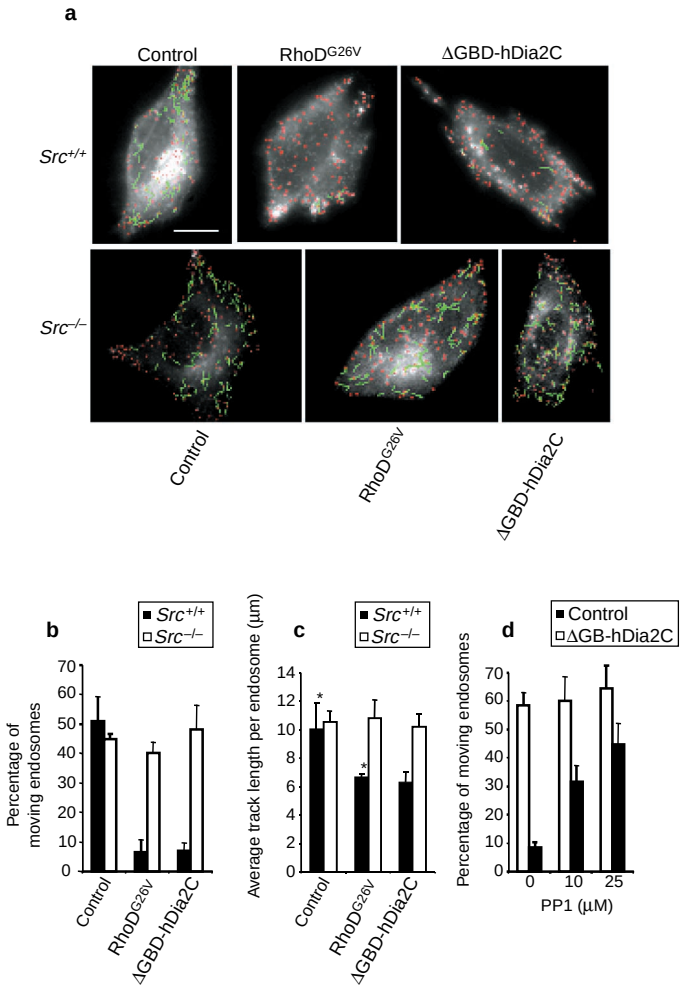

Figure 6 **RhoD/hDia2C regulate endosomes motility through Src kinase.** **a**, Motion Track 0.9. images representing GFP–Rab5-labelled endosomes (red open circles) and tracks (green lines) in *Src*$^{+/+}$ and *Src*$^{-/-}$ cells transfected with empty vector (control), or expressing RhoD^{G26V} or ΔGBD-hDia2C. Scale bar represents 10 μm. **b**, The reduction in motile endosomes induced by RhoD^{G26V} and ΔGBD-hDia2C is abolished in *Src*$^{-/-}$ cells. The histogram represents the percentage of motile endosomes of total detected. Error bars represent standard deviations. **c**, The average track length was calculated as in Fig. 3c. Asterisk, $P < 0.01$ when tested by Student's *t* test. **d**, The reduction in endosome motility induced by ΔGBD-hDia2C is abolished in *Src*$^{+/+}$ cells in a PP1 concentration-dependent manner. Quantification was performed as above.

for motility of GFP–Rab5-positive endosomes in response to expression of RhoD^{G26V} and ΔGBD-hDia2C (Fig. 6 and Table 2). Under basal conditions, a similar proportion of moving endosomes was detected in control *Src*$^{+/+}$ and *Src*$^{-/-}$ cells. Given the highly dynamic nature of this process[10], we cannot exclude the possibility that endosome movement may even be enhanced in *Src*$^{-/-}$ cells. Expression of RhoD^{G26V} and ΔGBD-hDia2C in *Src*$^{+/+}$ cells resulted in a blockage of endosome movement (83% and 88% of control, respectively; Fig. 6a, b), a decrease in track length and velocity of the moving vesicles (Fig. 6c and Table 2). This inhibitory effect, however, was not detected in *Src*$^{-/-}$ cells (Fig. 6 and Table 2) and was completely abolished by treatment with PP1 in *Src*$^{+/+}$ cells (Fig. 6d). Thus, expression of c-Src is required for the arrest of endosome motility induced by RhoD and hDia2C.

Discussion

We report here the identification of the first effector for RhoD, a novel Diaphanous protein, hDia2C, that induces a marked alignment of early endosomes along actin filaments and inhibits endosome motility through a mechanism requiring c-Src kinase activity. Our results provide a mechanistic function for the presence of RhoD, hDia2C and c-Src on early endosomes, by sequentially ordering them for the first time in a novel signalling pathway dedicated to the regulation of endosome motility. Importantly, these observations lead us to postulate the existence of a general mechanism that regulates the interaction of various cellular membrane compartments with the actin cytoskeleton. This hypothesis is based on the observation that the molecular pathway leading RhoD to activate c-Src kinase on endosomes through hDia2C shares mechanistic similarities to other Rho-dependent mechanisms occurring at the plasma membrane. A signalling pathway consisting of the sequential action of RhoA, mDia1 and Src has been shown to regulate the formation and maturation of focal contacts[38,39]. RhoD triggers a similar transduction pathway on endosomes, resulting in the interaction of this organelle with the actin cytoskeleton. As vesicular transport reactions depend on a common mechanism involving Rab GTPases, their effectors and SNAREs (SNAP receptors)[13], it is conceivable that membrane–cytoskeleton interactions underlying organelle positioning and motility may be generally regulated by

Rho–Dia–Src signalling cascades, similar to those observed for the plasma membrane and early endosomes. It is interesting in this respect that the machinery regulating early endosome motility involves a specific Rho family member and a specific hDia protein. The coding sequence of hDia2C is identical to hDia2B-12C[40] except for a sequence insertion and a deletion within the GBD[41]. Both sequences are encoded by separate and isolated exons, suggesting that *hDia2C* is a differentially spliced variant of the *hDIA2* gene. That such sequence variation changes the specificity of interaction with Rho GTPases is demonstrated by the binding of hDia2C, but not hDia2B, to RhoD and, in contrast to mDia1 and mDia2 (ref. 22), by its lack of interaction with RhoA or Cdc42. On this basis, we conclude that the GBD confers selectivity to hDia2C in the interaction with RhoD.

Consistent with hDia2C being a downstream effector of RhoD, the recruitment of hDia2C on early endosomes requires the GTP-dependent interaction with RhoD. Nonetheless, deletion of the GBD efficiently targets the mutant protein to endosomes in a RhoD-independent fashion. Thus, hDia2C has at least two determinants for the association with endosomes, the GBD for RhoD and sequences in the C-terminal region that are normally uncovered only after RhoD binding, but are constitutively exposed in the absence of the GBD. Similarly to RhoD, hDia2C decreases the velocity and displacement of endosomes. More strikingly, however, hDia2C renders these vesicles motionless. This poses the question of by what mechanism this occurs. Under physiological conditions, endosome movement is regulated by the interplay between actin filaments and microtubules[10]. Early endosomes accumulate in the juxtanuclear region after actin depolymerization, whereas loss of microtubules causes them to cluster in the sub-cortical region of the cell. Actin filaments and microtubules seem to support short- and long-range motility of endosomes, respectively. Rab5 and RhoD have distinct functions in these processes. Activation of Rab5 stimulates endosome motility along microtubules *in vivo* and *in vitro*[10]. The activity of microtubule motors enhanced by Rab5 and necessary for endosomes to move, tether and fuse with each other must evidently be counteracted by the RhoD–hDia2C pathway. In our experimental conditions, high levels of RhoD and hDia2C activity enhance the association of endosomes along actin filaments and thereby prevent the action of motors switching to microtubules. This would explain our previous results showing an extensive alignment of endosomes after expression of RhoD[17]. Under normal conditions, regulating the association of endosomes with actin, RhoD and hDia2C would modulate the balance between short- and long-range motility. Alternatively, the fact that treatment with Cytochalasin D did not completely rescue the RhoD/hDia2C-induced inhibitory effect suggests that RhoD/hDia2C may affect additional interactions that are important for organelle movement, such as negatively regulating a Rab5 effector essential for microtubule-based motility[10].

Regulation of interactions with the actin cytoskeleton is consistent with the established activity of Dia proteins. Formin proteins are thought to promote actin polymerisation by interacting with profilin[23,42] and, interestingly, they have recently been found to regulate nucleation and polarization of unbranched actin filaments[43], suggesting that hDia2C may promote actin assembly on the early endosome membrane. However, mDia proteins have recently also been shown to associate with microtubules, to stimulate the formation of stable detyrosinated microtubules in fibroblasts[44] and to co-align microtubules and actin bundles along the cell axis[34]. Here, we observed a similar reorganisation of actin filaments and microtubules after overexpression of both RhoD and hDia2C in HeLa cells. However, the activity of RhoD on endosome motility seems to be independent of its general effects on actin, that is, an increase in stress fibres and tubulin cytoskeleton. First, endosome movement is reduced after expression of RhoD in fibroblasts despite a decrease in actin stress fibres[17]. Second, that activated mDia1 mutant has no effect on endosome motility, suggesting that the activity of hDia2C is specific.

Further evidence in favour of an interaction with the actin cytoskeleton came from the finding that the RhoD/hDia2C pathway results in stimulation of c-Src kinase activity. FH proteins can interact directly with Src-homology 3 (SH3) domains of members of the Src non-receptor tyrosine kinase family through with their proline-rich FH1 region[35,45]. Our results suggest a new role for c-Src since the association of this kinase with endosomal membranes was reported a decade ago[36] and provide a new function to the previously observed colocalization between mDia1, 2 and c-Src on endosomes in HeLa cells[35]. The finding that c-Src activity is stimulated after recruitment to early endosomes highlights a mechanism whereby protein localization modulates its signalling functions. Moreover, formin (Limb deformity protein) interacts with c-Src on perinuclear membranes in primary mouse fibroblasts[45]. One question concerns the role of c-Src in this process. Tyrosine phosphorylation by c-Src may modify the properties of proteins that regulate actin polymer dynamics. For example, Cortactin is a substrate of c-Src[46] that enhances the ability of the Arp2/3 complex to assemble branched actin filament networks[47].

The RhoD–hDia2C–Src pathway may be important during cell division. RhoD is involved in cytokinesis[48], raising the question of a potential link with endosome dynamics. The general arrest of membrane traffic during cell division includes endocytosis[49]. Endosomes tend to cluster at the mitotic spindle pole[36], where mDia1 is also localized[50], before partitioning between the daughter cells[51]. The mechanism by which RhoD interferes with cytokinesis may involve interactions of endosomal vesicles with microtubules and actin. Our observations suggest testable hypotheses that should provide novel insights into membrane cytoskeleton interactions both in interphase and during cell division. □

Methods

Antibodies, plasmids and other reagents

Anti-HA and anti-Src antibodies were purchased from Santa Cruz Biotechnology (Santa Cruz, CA), anti-Flag antibodies from Upstate Biotechnology (Charlottesville, VA), secondary antibodies conjugates (horseradish peroxidase and fluorescently labelled) from Dianova (Hamburg, VA). Construction of plasmids and cloning were made by standard procedures and are available on request. RhoDΔCCLAT cloned into pLexA2 was a gift from H. McBride (Ottowa, University of Ottowa Heart Institute, Canada), pEGFP-hRab5 (ref. 10) has previously been described, Flag-mDia1 and ΔN3-mDia1 were a gift from S. Narumiya (Kyoto University Faculty of Medicine, Japan), pCMV-HA-hDia2B was from D. Tonolio (Genetic Molecular Institute CNR, Pavia, Italy), pEGFP-SrcWT and pEGFP-Src^{Y527F} was a gift from G. Superti-Fuga (EMBL, Heidelberg, Germany). BlastN and TblastN searches against the human EST database resulted in the accession numbers BG53234.2; BF590974.1; AA907630.1; AW408745.1 for the EST containing the deletion following amino-acid 42 of human Dia2-12C and -156 and no. AW962735.1; AA315818.1; AW962743.1; BG503061.1 and BF899139.1 for the EST containing the insert at position 149. The primers used for cloning the remaining 5′ end of *hDia2C* (5′-ACCCGTAACTTTACTTCCAACTAT-3′ and 5′-CGGAATTCCATGGAGCAGCCCGGGGCGG-3′) were purchased from Sigma-ARK (Steinheim, Germany). The mixture of antipain, pepstatin A, leupeptin, chymostatin, aprotinin and α-phenylmethyl sulphonyl fluoride (PMSF) protease inhibitors was purchased from Sigma.

Recombinant proteins

DH5α *Escherichia coli* transformed with pGEX2T-RhoD wild type were grown in M9 minimal culture medium for 8 h at 37 °C. Expression of GST–RhoD was then induced in the presence of 0.1 mM IPTG for 8 h at 37 °C. The protein was purified on glutathione–Sepharose 4B beads (Pharmacia, Freiburg, Germany) as previously described[29] and cleaved with thrombin to separate the RhoD protein from GST.

siRNA preparation and transfection

Duplex siRNA homologous to *hDia2C* and *GFP* (*HDia2C* oligonucleotides were 5′-UCUAUAGUUGGAAGUAAAGdTdT-3′ and 5′-CUUUACUUCCAACUAUAGAdTdT-3′; GFP oligonucleotides were 5′-GGAGCGCACCAUCUUCUUCdTdT-3′ and 5′-GAAGAAGAUGGUGCGCUCCdTdT-3′) designed as described[33], were purchased from ProLigo (Paris, France). dsRNA oligonucleotides were transfected with Oligofectamine or Lipofectamine 2000 (Invitrogen, Carlsbad, CA) when combined with plasmid DNA.

Antibody production

A peptide, SEFPAAQPLYDERSLNLSEK, corresponding to the sequence 74–93 of hDia2C was synthesized and injected into rabbits (Sigma Genosys Ltd, Cambridge, England). Recombinant RhoD protein was injected into rabbits with Ribi adjuvant (– MPL + TDM + CWS; Ribi Immunogen research Inc., Hamilton, MA). Anti-RhoD serum was affinity purified using recombinant RhoD immobilized on

Sulfolink beads (Pierce Chemical Company, Rockford, IL)

Two-hybrid screening

The yeast reporter strain L40 (*MATa trp1 leu2 his3 LYS::lexA-HIS3 URA3::LexA-lacZ*) was transformed with pLexA-RhoD^{G26V} ΔCCLAT using a lithium acetate-based method and grown on synthetic medium lacking tryptophan. This transformant was then transformed with library DNA (MATCHMAKER HeLa cell oligo(dT)-primed library in pGADGH; Clonetech, Heidelberg, Germany). The transformants were grown for 3 h in synthetic medium lacking tryptophan and leucine and plated on synthetic medium lacking histidine, leucine, tryptophan, uracil and lysine. Colonies were picked 4.5 days after plating and tested for β-galactosidase activity using a replica filter and a liquid assays. Library plasmids from positive clones were rescued into *E. coli* HB101 cells plate on leucine-free medium and subsequently analysed by DNA sequencing.

Cell culture, transfection and immunofluorescence

HeLa cells were grown in MEM containing 5% heat-inactivated foetal calf serum (FCS), 100U ml^{-1} penicillin, 100 μg ml^{-1} streptomycin, 2 mM L-glutamine and non-essantial amino acids. *Src*$^{-/-}$ cells were derived from knock-out mice embryo and immortalized by infection with a retroviral vector transducing the SV40 large T antigen[37]. They were grown in DMEM containing 10% heat-inactivated FCS, 100 U ml^{-1} penicillin, 100 μg ml^{-1} streptomycin and 2 mM L-glutamine.

For transient expression studies, HeLa cells were transfected with plasmids containing DNA of interest using Effectene (Qiagen, Hilden, Germany) or Fugene (Boeringer, Manheim, Germany). Cells were analysed 24 h post-transfection. Immunofluorescence labelling was performed according to standard procedures. For transferrin internalization, cells were serum starved for 1 h before incubation with 50 μg ml^{-1} Alexa-568-labelled transferrin (Molecular Probes, Eugene, OR).

In vitro binding assays, immunoprecipitation and *in vitro* translation

GST–RhoD affinity chromatography was performed as for Rab5 (ref. 52). The proteins eluted from the beads complexed with either GST–RhoD-GDP or GST–RhoD-GTP-γS were resuspended in sample buffer, boiled for 5 min at 95 °C, separated by SDS–polyacrylamide gel electrophoresis (PAGE), blotted onto nitrocellulose and probed with anti-hDia2 peptide antibodies, before detection by ECL detection (Amersham). For immunoprecipitation, HeLa cells grown in 10-cm dishes were transfected as described above. After 24 h of transfection, cells were washed with ice-cold PBS and lysed in 20 mM Tris-HCl at pH 7.4, 1% Triton X-100, 5 mM magnesium chloride, 150 mM sodium chloride, 0.1 mM dithiothreitol (DTT) and a mixture of protease inhibitors. The lysate was centrifuged at 15,000*g* for 10 min and the supernatant was incubated with either pre-immune or anti-RhoD serum, or purified mouse 9E10 anti-Myc monoclonal antibodies at 4 °C for 1 h. Protein A–agarose (20 μl; Santa Cruz Biotechnology) were then added and the incubation was continued for 1 h at 4 °C. Beads were then washed five times with lysis buffer, resuspended in sample buffer and boiled for 5 min at 95 °C. Immunoprecipitates were analysed by SDS–PAGE, blotted onto nitrocellulose and probed with the indicated antibodies, before ECL detection (Amersham). ^{35}S-Methionine-labelled proteins were transcribed and translated *in vitro* using a TnT coupled transcription–translation kit (Promega, Manheim, Germany).

Live cell imaging

HeLa cells grown in 11-mm glass coverslips were cotransfected with hRab5–GFP and plasmids containing the DNA of interest. After 24 h of transfection, cell imaging was performed in CO_2-independent medium (Invitrogen). Time-lapse series were acquired at 37 °C on an inverted Olympus IX70 microscope equipped with a 100× oil immersion objective, NA 1.35, and a 12-bit Till Imago CCD camera (Till Photonics, Gräfelfing, Germany). The temperature was controlled by a climate box covering the apparatus. 100 frames were captured at 300-ms intervals.

Image processing and quantification of endosome motility

Time-lapse image series were exported as single TIFF files and processed in Object-image 2.5 to be converted into QuickTime movies. Endosome motility was analysed and quantified using the Motion Track program version 0.9 (Kalaidzidis, Y., unpublished observations). The Motion Track program was built on a Pluk platform[53] and includes a vesicle finding module, a tracking module, a track-seaming module and a random motion elimination module. The vesicle finding module was built on the basis of a stratified erosion algorithm, which allows separation of bright particles from a noisy non-constant-intensity surrounding. The tracking module is based on a previously described algorithm[54] and uses a score function handling non-flow-like movement in the cell. The track-seaming module partially decreases the number of low signal-to-noise ratio-induced broken tracks. The random motion elimination module calculates non-smoothness of trajectory and eliminates random trajectory movement. This module excludes Brownian motion, noise and sampling error. The images of endosomes tracks illustrate the distance over which the vesicles are moving. These are merged images generated by the program from a stack of 100 frames collected at 300-ms intervals. The average track length of moving endosomes represents the ratio between measured total track length and the number of moving endosomes detected.

Src activity assay

The Src kinase activity was measured using Src Assay kit provided by Upstate Biotechnology. The assay is based on phosphorylation of the specific KVEKIGEGTYGVVYK peptide substrate. The phosphorylated substrate is then separated from residual γ-^{32}P-ATP using p81 phosphocellulose paper and quantified with a scintillation counter. Background measured in the absence of Src substrate was subtracted.

RECEIVED 17 JUNE 2002; REVISED 19 NOVEMBER 2002; ACCEPTED 3 JANUARY 2003; PUBLISHED 10 FEBRUARY 2003.

1. Mellman, I. Endocytosis and molecular sorting. *Annu. Rev. Cell Dev. Biol.* **12,** 575–625 (1996).
2. Kubler, E. & Riezman, H. Actin and fimbrin are required for the internalization step of endocytosis in yeast. *EMBO J.* **12,** 2855–2862 (1993).
3. Fujimoto, L. M., Roth, R., Heuser, J. E. & Schmid, S. L. Actin assembly plays a variable, but not obligatory role in receptor-mediated endocytosis in mammalian cells. *Traffic* **1,** 161–171 (2000).
4. Buss, F., Arden, S. D., Lindsay, M., Luzio, J. P. & Kendrick-Jones, J. Myosin VI isoform localized to clathrin-coated vesicles with a role in clathrin-mediated endocytosis. *EMBO J.* **20,** 3676–3684 (2001).
5. Durrbach, A., Louvard, D. & Coudrier, E. Actin filaments facilitate two steps of endocytosis. *J. Cell Sci.* **109,** 457–465 (1996).
6. Raposo, G. *et al.* Association of myosin I α with endosomes and lysosomes in mammalian cells. *Mol. Biol. Cell* **10,** 1477–1494 (1999).
7. Taunton, J. Actin filament nucleation by endosomes, lysosomes and secretory vesicles. *Curr. Opin. Cell Biol.* **13,** 85–91 (2001).
8. Matteoni, R. & Kreis, T. E. Translocation and clustering of endosomes and lysosomes depends on microtubules. *J. Cell Biol.* **105,** 1253–1265 (1987).
9. McGraw, T. E., Dunn, K. W. & Maxfield, F. R. Isolation of a temperature-sensitive variant Chinese hamster ovary cell line with a morphologically altered endocytic recycling compartment. *J. Cell Physiol.* **155,** 579–594 (1993).
10. Nielsen, E., Severin, F., Backer, J. M., Hyman, A. A. & Zerial, M. Rab5 regulates motility of early endosomes on microtubules. *Nature Cell Biol.* **1,** 376–382 (1999).
11. Aniento, F., Emans, N., Griffiths, G. & Gruenberg, J. Cytoplasmic dynein-dependent vesicular transport from early to late endosomes. *J. Cell Biol.* **123,** 1373–1387 (1993).
12. Bomsel, M., Parton, R., Kuznetsov, S. A., Schroer, T. & Gruenberg, J. Microtubule- and motor-dependent fusion *in vitro* between apical and basolateral endocytic vesicles from MDCK cells. *Cell* **62,** 719–731 (1990).
13. Zerial, M. & McBride, H. Rab proteins as membrane organizers. *Nature Rev. Mol. Cell Biol.* **2,** 107–117 (2001).
14. Ridley, A. J. Rho proteins: linking signaling with membrane trafficking. *Traffic* **2,** 303–310 (2001).
15. Lamaze, C., Chuang, T.-H., Terlecky, L. J., Bokoch, G. M. & Schmid, S. L. Regulation of receptor-mediated endocytosis by Rho and Rac. *Nature* **382,** 177–179 (1996).
16. Kroschewski, R., Hall, A. & Mellman, I. Cdc42 controls secretory and endocytic transport to the basolateral plasma membrane of MDCK cells. *Nature Cell Biol.* **1,** 8–13 (1999).
17. Murphy, C. *et al.* Endosome dynamics regulated by a novel rho protein. *Nature* **384,** 427–432 (1996).
18. Gampel, A., Parker, P. J. & Mellor, H. Regulation of epidermal growth factor receptor traffic by the small GTPase RhoB. *Curr. Biol.* **9,** 955–958 (1999).
19. Bishop, A. L. & Hall, A. Rho GTPases and their effector proteins. *Biochem J.* **348,** 241–255 (2000).
20. Evangelista, M. *et al.* Bni1p, a yeast formin linking cdc42p and the actin cytoskeleton during polarized morphogenesis. *Science* **276,** 118–122 (1997).
21. Kohno, H. *et al.* Bni1p implicated in cytoskeletal control is a putative target of Rho1p small GTP binding protein in *Saccharomyces cerevisiae*. *EMBO J.* **15,** 6060–6068 (1996).
22. Alberts, A. S., Bouquin, N., Johnston, L. H. & Treisman, R. Analysis of RhoA-binding proteins reveals an interaction domain conserved in heterotrimeric G protein β subunits and the yeast response regulator protein Skn7. *J. Biol. Chem.* **273,** 8616–8622 (1998).
23. Watanabe, N. *et al.* p140mDia, a mammalian homolog of *Drosophila* diaphanous, is a target protein for Rho small GTPase and is a ligand for profilin. *EMBO J.* **16,** 3044–3056 (1997).
24. Westendorf, J. J. The formin/diaphanous-related protein, FHOS, interacts with Rac1 and activates transcription from the serum response element. *J. Biol. Chem.* **276,** 46453–46459 (2001).
25. Yayoshi-Yamamoto, S., Taniuchi, I. & Watanabe, T. FRL, a novel formin-related protein, binds to Rac and regulates cell motility and survival of macrophages. *Mol. Cell Biol.* **20,** 6872–6881 (2000).
26. Wasserman, S. FH proteins as cytoskeletal organizers. *Trends Cell Biol.* **8,** 111–115 (1998).
27. Tanaka, K. Formin family proteins in cytoskeletal control. *Biochem. Biophys. Res. Commun.* **267,** 479–481 (2000).
28. Rutherford, K. *et al.* Artemis: sequence visualization and annotation. *Bioinformatics* **16,** 944–945 (2000).
29. Chistoforidis, S., McBride, H. M., Burgoyne, R., D. & Zerial, M. The Rab5 effector EEA1 is a core component of endosome docking. *Nature* **397,** 621–625 (1999).
30. Watanabe, N., Kato, T., Fujita, A., Ishizaki, T. & Narumiya, S. Cooperation between mDia1 and ROCK in Rho-induced actin reorganization. *Nature Cell Biol.* **1,** 136–143 (1999).
31. Murphy, C. *et al.* Dual function of RhoD in vesicular movement and cell motility. *Eur. J. Cell Biol.* **80,** 391–398 (2001).
32. Sonnichsen, B., De Renzis, S., Nielsen, E., Rietdorf, J. & Zerial, M. Distinct membrane domains on endosomes in the recycling pathway visualized by multicolor imaging of Rab4, Rab5, and Rab11. *J. Cell Biol.* **149,** 901–914 (2000).
33. Elbashir, S. M. *et al.* Duplexes of 21-nucleotide RNAs mediate RNA interference in cultured mammalian cells. *Nature* **411,** 494–498 (2001).
34. Ishizaki, T. *et al.* Coordination of microtubules and the actin cytoskeleton by the Rho effector mDia1. *Nature Cell Biol.* **3,** 8–14 (2001).
35. Tominaga, T. *et al.* Diaphanous-related formins bridge Rho GTPase and Src tyrosine kinase signaling. *Mol. Cell* **5,** 13–25 (2000).
36. Kaplan, K. B., Swedlow, J. R., Varmus, H. E. & Morgan, D. O. Association of p60c-src with endosomal membranes in mammalian fibroblasts. *J. Cell Biol.* **118,** 321–333 (1992).
37. Klinghoffer, R. A., Sachsenmaier, C., Cooper, J. A. & Soriano, P. Src family kinases are required for integrin but not PDGFR signal transduction. *EMBO J.* **18,** 2459–2471 (1999).
38. Riveline, D. *et al.* Focal contacts as mechanosensors: externally applied local mechanical force induces growth of focal contacts by an mDia1-dependent and ROCK- independent mechanism. *J. Cell Biol.* **153,** 1175–1186 (2001).
39. Volberg, T., Romer, L., Zamir, E. & Geiger, B. pp60(c-src) and related tyrosine kinases: a role in the assembly and reorganization of matrix adhesions. *J. Cell Sci.* **114,** 2279–2289 (2001).
40. Bione, S. *et al.* A human homologue of the *Drosophila melanogaster diaphanous* gene is disrupted in a patient with premature ovarian failure: evidence for conserved function in oogenesis and implications for human sterility. *Am. J. Hum. Genet.* **62,** 533–541 (1998).
41. Krebs, A., Rothkegel, M., Klar, M. & Jockusch, B. M. Characterization of functional domains of mDia1, a link between the small GTPase Rho and the actin cytoskeleton. *J. Cell Sci.* **114,** 3663–3672 (2001).
42. Evangelista, M., Pruyne, D., Amberg, D. C., Boone, C. & Bretscher, A. Formins direct Arp2/3-independent actin filament assembly to polarize cell growth in yeast. *Nature Cell Biol.* **4,** 32–41 (2002).

43. Pruyne, D. *et al.* Role of formins in actin assembly: nucleation and barbed-end association. *Science* **297,** 612–615 (2002).
44. Palazzo, A. F., Cook, T. A., Alberts, A. S. & Gundersen, G. G. mDia mediates Rho-regulated formation and orientation of stable microtubules. *Nature Cell Biol.* **3,** 723–729 (2001).
45. Uetz, P., Fumagalli, S., James, D. & Zeller, R. Molecular interaction between limb deformity proteins (formins) and Src family kinases. *J. Biol. Chem.* **271,** 33525–33530 (1996).
46. Wu, H., Reynolds, A. B., Kanner, S. B., Vines, R. R. & Parsons, J. T. Identification and characterization of a novel cytoskeleton-associated pp60src substrate. *Mol. Cell Biol.* **11,** 5113–5124 (1991).
47. Uruno, T. *et al.* Activation of Arp2/3 complex-mediated actin polymerization by cortactin. *Nature Cell Biol.* **3,** 259–266 (2001).
48. Tsubakimoto, K. *et al.* Small GTPase RhoD suppresses cell migration and cytokinesis. *Oncogene* **18,** 2431–2440 (1999).
49. Warren, G. Membrane partitioning during cell division. *Annu. Rev. Biochem.* **62,** 323–348 (1993).
50. Kato, T. *et al.* Localization of a mammalian homolog of diaphanous, mDia1, to the mitotic spindle in HeLa cells. *J. Cell Sci.* **114,** 775–784 (2001).
51. Bergeland, T., Widerberg, J., Bakke, O. & Nordeng, T. W. Mitotic partitioning of endosomes and lysosomes. *Curr. Biol.* **11,** 644–651 (2001).
52. Christoforidis, S. & Zerial, M. Purification and identification of novel Rab effectors using affinity chromatography. *Methods* **20,** 403–410 (2000).
53. Kalaidzidis, Y. L., Gavrilov, A. V., Zaitsev, P. V., Kalaidzidis, A. L. & Korolev, E. V. Pluk a software development environment programming. *Programmirovanie* **4,** 38–46 (1997).
54. Chetverikov, D. & Verestói, J. Feature point tracking for incomplete trajectories. *Computing* **62,** 321–338 (1999).

ACKNOWLEDGEMENTS
We are grateful to S. Narumiya for providing pFL-mDia1 and pFL-mDia1ΔN3, H. McBride for pLexA-RhoD^{G26V} (–CAAX) and D. Toniolo for pCMV-HA-hDia2B. We acknowledge the generosity of P. Soriano and G. Superti-Furga for kindly providing *Src*$^{+/+}$ and *Src*$^{-/-}$ cell lines, as well as pEGFP-SrcWT and pEGFP-SrcY527F. Special thanks A. Desay, J. Howard, H. Mellor, C. Murphy and J. Rink for valuable discussions and comments on the manuscript, and to S. Chasserot-Golaz for help with confocal microscopy. We would like also to thank A. Giner for technical assistance, B. Habermann for biocomputing analysis and D. Bagnard for sharing technical resources. This work was supported by a Human Frontier Science Program (HFSP) long-term fellowship to S.G. (LT0493/1999-M) and by a HFSP grant to M.Z. (RG0260/1999-M)
Correspondence and requests for material should be addressed to M.Z.
Supplementary Information accompanies the paper on www.nature.com/naturecellbiology.

COMPETING FINANCIAL INTERESTS
The authors declare that they have no competing financial interests.

All videos were acquired and processed as described previously in Live Cell Imaging and Image Processing. They comprise 100 frames, animated at 20 frames/s (around 7 × acquisition time).

Movie 1 HeLa cells co-overexpressing hRab5-GFP and empty pCDNA3.1.

Movie 2 HeLa cells co-overexpressing hRab5-GFP and $RhoD^{V26}$.

Movie 3 HeLa cells co-overexpressing hRab5-GFP and ΔGBD-hDia2C.

Supplementary information

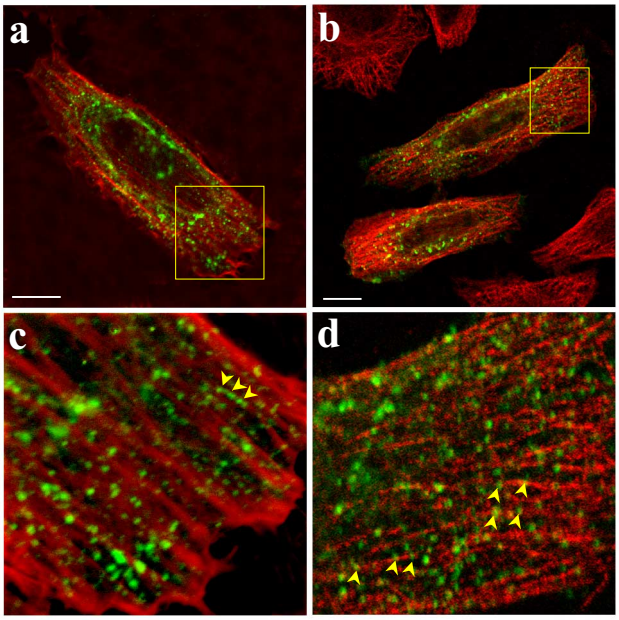

Figure S1. mDia1 do not regulate endosome-cytoskeleton interactions

a-d, *Endosome alignment along actin and tubulin filaments in cells expressing ΔN3-mDia1.* Hela cells were co-transfected with Flag-ΔN3-mDia1 and Rab5-GFP. After 24hrs, cells were processed for immunofluorescence and analysed by confocal microscopy. Cells expressing Flag-ΔN3-mDia1 were detected with an anti-Flag antibodies followed by CY5-conjugated anti-mouse antibodies (not shown). F-actin was visualized by staining with TRITC-conjugated phalloidin (a, c). Microtubules were detected with anti-β-tubulin antibodies followed by CY3-conjugated goat anti-mouse (b, d). c and d represent higher magnification of the region framed in a and b, respectively. The arrows in c and d represent linear tracks of Rab5-endosomes associating with actin filaments and microtubules, respectively. Note that cell expressing ΔN3-mDia1 display a lower proportion of endosomes aligned along actin filaments (see quantification in Fig. 4e). Scale bar represent 10 μm.